P8.4

MISOCYCLONE DETECTION AND OBSERVATIONS USING THE WSR-88D: OPERATIONAL IMPLICATIONS FOR THE WARNING METEOROLOGIST

Albert E. Pietrycha*
National Weather Service, Goodland, Kansas

Kevin L. Manross
National Severe Storm Laboratory, Norman, Oklahoma

Eric Nelson
National Center for Atmospheric Research, Boulder, Colorado

1. INTRODUCTION

The detection of non-mesocyclone tornadoes (Szoke and Brady 1989) with the Weather Surveillance Radar-1988 Doppler (WSR-88D; Crum and Alberty 1993) is one of the most challenging meteorological phenomena for an operational meteorologist. Numerous observational and numerical research efforts (Wilson 1986; Wilson et al. 1988; Szoke and Brady 1989; Wakimoto and Wilson 1989; Wilczak and Christian 1990; Wilson et al. 1992, Lee and Wilhelmson 1997, and numerous others) have addressed various theories behind the development of misocyclones (Fujita 1981) and non-mesocyclone tornadoes. However, to date, few operationally relevant studies have specifically examined WSR-88D data to address the detection of preexisting vortices prior to and during the development of the non-mesocyclone tornadoes. When sufficient scatterers are present within the boundary layer, the WSR-88D can resolve misocyclones with adequate temporal resolution to enhance a warning forecaster's situational awareness and improve warning lead time on tornado warnings associated with non-mesocyclone tornadoes.

Three cases are presented within, two of which focus on the Denver Convergence-Vorticity Zone (e.g., Szoke et al. 1984; Szoke and Brown 1987; Wilczak and Glendening 1988) (DCVZ; 04 October 2004, 23 July 1998) and one event that occurred in Nebraska on 02 July 2002 along a surface trough of low pressure. WSR-88D data resolved coherent vortices, embedded within those surface boundaries and in several examples were identifiable in the radar data up to 120 minutes prior to tornadogenesis, exhibited horizontal diameters of 1 to 4 km, vertical depths up to 3 km above radar level (ARL), and exhibited the well documented lobe and cleft pattern (Carbone 1982, Wilson 1986, Mueller and Carbone 1987, Wakimoto and Wilson 1989) reflectivity and velocity signatures. Vortex mergers were also resolved as well as collocation of vortices with larger parent tornadic circulations that ascended with height.

Corresponding author address: Albert Pietrycha, 920 Armory Rd, Goodland, KS 67735; albert.pietrycha@noaa.gov

2. METHODOLOGY

A thorough case study presentation associated with each event is beyond the specific scope of this paper. However, detailed plan view and cross-sectional analyses of radar data, high spatial resolution of surface data, upper air and satellite data were performed in order to ensure our understanding of the evolution with each case discussed. Level-II radar data (Crum et al. 1993) were utilized for all radar imagery depicted within. Fortuitously, with the 4 October 2004 case, video and audio footage taken from two television helicopters provided accurate location and time information of the tornadoes, thereby allowing accurate correlation with the radar data. Similarly, for the 23 July 1998 case, visual observations of the tornadoes from the sub-VORTEX (Verifying the Origins of Rotation in Tornadoes Experiment) (Rasmussen et al. 1994) crew allowed for accurate correlation with the radar data.

3. DATA

a) 4 October 2004

On the late afternoon of 4 October 2004, northwest of the Denver International Airport eleven non-mesocyclone tornadoes developed along a DCVZ in northeast Colorado (*Storm Data* 2004). The tornadoes occurred within a 44 minute period between 2204 to 2248 UTC with the four strongest tornadoes producing F1 damage. The tornadoes developed in the vicinity of a triple point where the DCVZ intersected an in situ outflow boundary. The outflow boundary was generated by intensifying deep moist convection located along and immediately east of the DCVZ. Vortex evolution through the time period of the first three tornadoes is discussed below.

As early as 1700 UTC the Front Range WSR-88D (KFTG) resolved the reflective gradient (radar fine-line) associated with the DVCZ. Throughout the afternoon the boundary was oriented generally north-northeast to south-southwest and remained quasi-stationary. At 2045 UTC, 1.25 hours prior to the first tornado, the first in a series of vortices was resolved in the base velocity data embedded within the DCVZ, located within 10 km west northwest of the radar; vortex A and B. Vortex A and B were separated by a distance of 11 km and propagated north at ~4 m s^{-1} (Fig. 1).

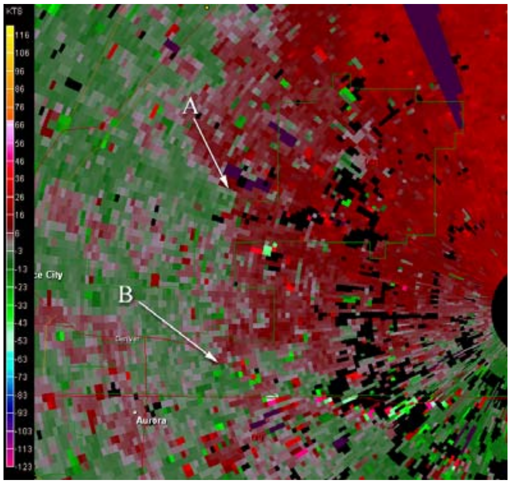

Fig. 1. KFTG 0.5° base velocity, valid at 2045 UTC 4 October 2004. The location of Vortex A and B denoted by white arrows.

Based on cross-sectional imagery (not shown), vortex A and B were shallow in depth, under 2 km ARL, with no detectable cloud mass above either vortex. Maximum radial shear was ~20 m s^{-1}, a typical value for all the vortices discussed for this case. Additionally, by 2115 UTC a smaller diameter vortex (A') developed between vortex A and B (Fig. 2). Vortex A' appeared to merge with vortex A prior to 2130 UTC (Fig. 3). No appreciable change in vortex diameter, depth or strength of the velocity couplet was resolved in the radar data after the merger. Furthermore, at 2115 UTC vortex C was resolved in the base velocity data (Fig. 2). Similar to vortices A and B, the vertical depth of vortex C was less than 2 km. Of interest, for the remainder of the event, a lobe and cleft or, rather, an "*S*" shaped pattern associated with the train of misocyclones along the DCVZ was resolved in the base velocity data.

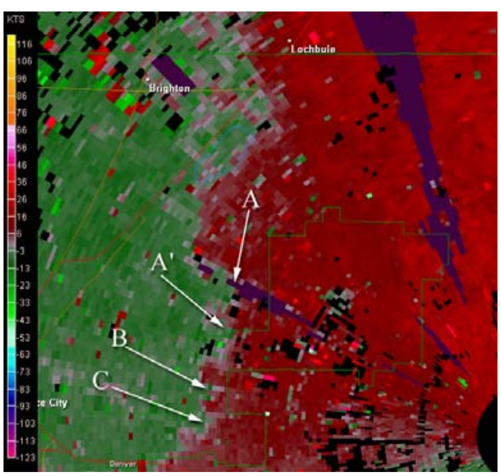

Fig. 2. As in Fig. 1 except for 2115 UTC 4 October 2004.

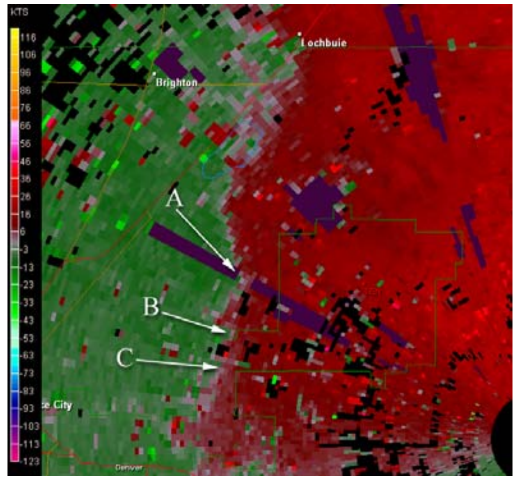

Fig. 3. As in Fig. 1 except for 2130 UTC 4 October 2004.

Between 2130 to 2145 UTC, cloud mass was detected above vortex A concurrent with an increase in the height of the vortex from 2 km to 4.1 km ARL (Fig. 4a). The increase in height occurred at the time when reflectivity aloft, up to 47 dBZ, developed above the vortex (Fig 4b). The rapid ascent of the vortex concurrent with developing echoes aloft suggests the vortex became coupled with a rapidly developing updraft (Fig. 4b).

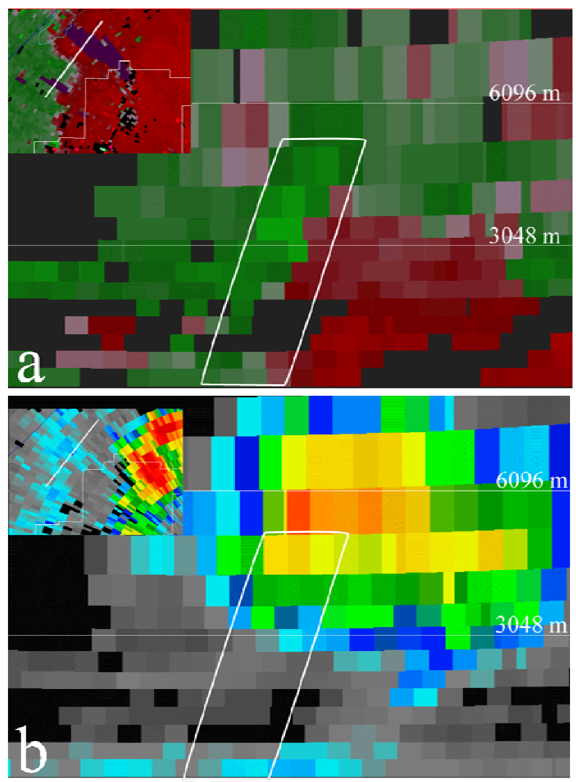

Fig. 4. (a) KFTG base velocity cross section for 2145 UTC 4 October 2004. The white parallelogram denotes the location of the vortex. Height scale (horizontal white line) labeled every 3048 m. (b) as in (a) except depicting base reflectivity.

Based on video and eyewitness accounts by two TV news helicopter crews, the first of three tornadoes developed at 2204 UTC and persisted for 10 minutes. The tornado was located in the vicinity of the terminus of the DCVZ with the outflow boundary, coincident with the location of vortex A (Fig. 5). Over the next 10 minutes, vortex A translated northwest along the outflow boundary at ~4 m s^{-1}. The tornado dissipated by 2215 UTC, coincident with the demise of the base velocity couplet associated with the parent circulation. Reportedly, a second tornado occurred simultaneously with, and in very close proximity to, the first tornado. The exact time and location of the second tornado is unknown but apparently the tornado was brief in duration. A differential velocity signature associated with the second tornado was not resolved in the base velocity data. Additionally, by 2215 UTC vortex C merged into the circulation associated with vortex B (Fig. 6). Vortex D was now resolved the velocity data with a vertical depth under 2 km ARL (Fig. 6).

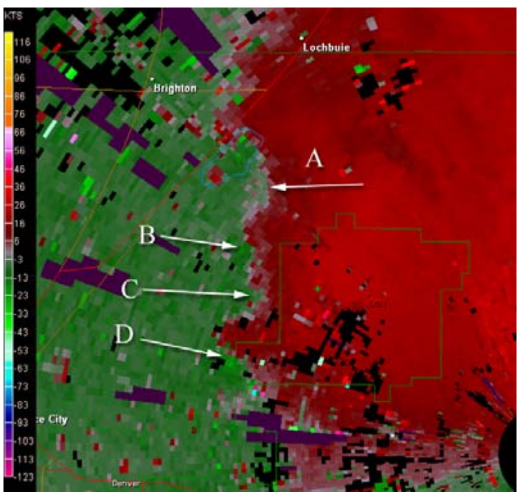

Fig. 5. As in Fig. 1 except for 2200 UTC 4 October 2004.

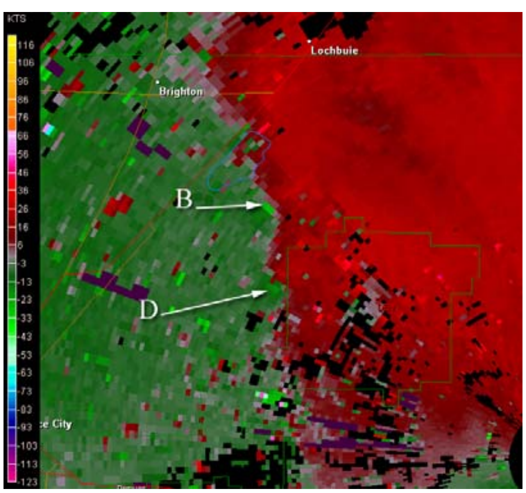

Fig. 6. As in Fig. 1 except for 2215 UTC 4 October 2004.

Through 2220 UTC vortex B and vortex D translated north along the DCVZ at ~4 m s^{-1} with vortex B approaching the triple point. By 2220 UTC vortex B became collocated with the parent updraft that produced the previous two tornadoes, concurrent at the time when the third tornado was reported. Similar to the motion of vortex A at the time of the first tornado, vortex B moved toward the northwest along the outflow boundary. The third tornado persisted until ~2230 UTC, coincident when the velocity couplet associated with vortex B was no longer identifiable in the base velocity data (Fig. 7). At 2230 UTC, vortex D translated north to the location of the triple point (Fig. 7). No tornado could be associated with vortex D. Forward from this point in time, a renewed surge of outflow moved west over taking the portion of the DCVZ immediately northwest of the Denver International Airport, closing the window for tornadoes along that portion of the DCVZ.

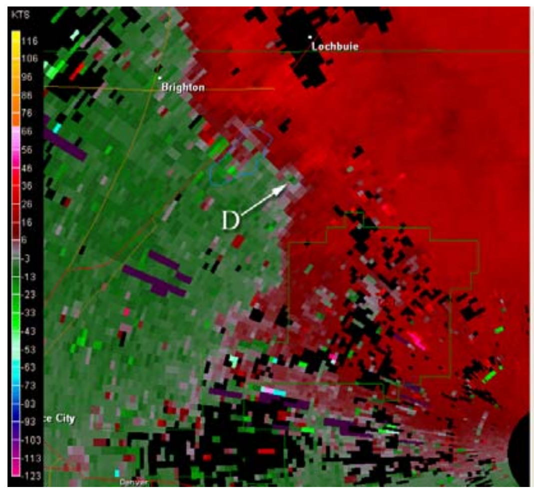

Fig. 7. As in Fig. 1 except for 2229 UTC 4 October 2004.

b) 02 July, 2002

On the early evening of 5 October 2004, two F0, non-mesocyclone tornadoes developed along a surface trough of low pressure in Brown County, located in north central Nebraska (*Storm Data* 2002). Pietrycha and Manross (2003) documented cyclonic vortices embedded with a surface trough of low pressure, identifiable in the North Platte, Nebraska WSR-88D (KLNX) base radar products within 85 km of the radar (see their Fig. 2). Reflectivity and velocity cross-sectional analysis indicated the vortices sloped with height toward the northeast, similar to the orientation of the boundary, while exhibiting a coherent structure up to a height of 3.5 km ARL. The circulations exhibited 3-6 km horizontal diameters, with a wavelength of ~12 km. The largest vortices persisted over 120 min as they propagated along the boundary at ~5 m s^{-1}. The maximum radial shear associated with a vortex prior to convection initiation was 23 m s^{-1} across a distance of 1.5 km. Discussed but not shown in their paper was that over time, several of the circulations ascended within the parent updrafts. A velocity cross section of their vortex #5 (see their Fig. 5) is shown in Fig.8.

Rapid growth in an updraft collocated with vortex #5 was underway by 0022 UTC. Plan view and cross-sectional analysis resolved the vortex to a height of ~3 km ARL (Fig. 8). The maximum radial shear associated with a vortex was 19 m s^{-1} across a distance of 1 km, at 908 m ARL. Over the next 35 minutes, the vortex ascended within the parent updraft to a height of ~9 km ARL (Fig. 9). At 0100 UTC, the time of maximum vortex ascent and radial shear, the radial shear associated with the vortex was 42 m s^{-1} across a distance of 1 km, at 8.4 km ARL. It remains unclear whether vortex #5 was associated with either of the two F0 tornadoes that were reported in Brown County, Nebraska associated with this case.

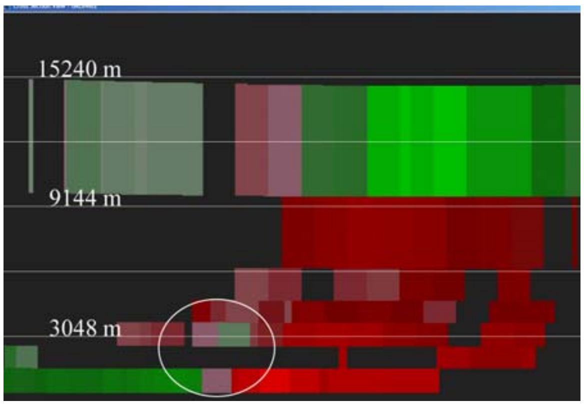

Fig. 8. Base velocity cross section from KLNX for 0022 UTC 3 July 2002. The white circle denotes the circulation associated with the vortex. Height interval as in Fig. 4.

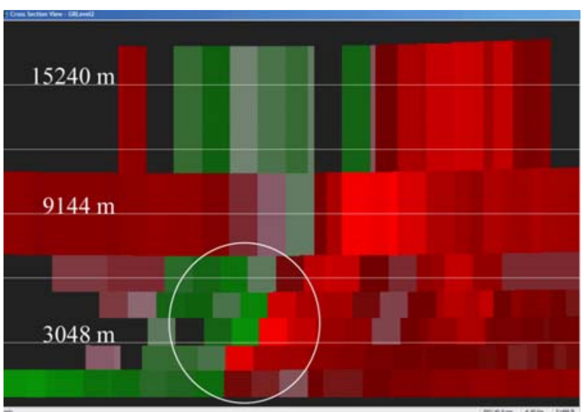

Fig. 9. As in Fig. 8 except for 0100 UTC 3 July 2002.

c) 23 July, 1998

On the afternoon of 23 July 1998, two non-mesocyclone tornadoes were observed by the sub-VORTEX team in northeast Colorado, ~40 km east of the KFTG WSR-88D. The deep moist convection supporting the tornadoes initiated on the DCVZ. At 2130 UTC, 23 minutes before the first tornado, the velocity couplet associated with the vortex that would ultimately become entrained into the parent tornadic circulation was resolved, embedded within the DCVZ (Fig. 10). Radial velocity data resolved the circulation through a height of ~2.0 km ARL with a diameter of no more than 0.75 km. A developing updraft existed ~4 km east of the vortex with a reflective core maximum of 20 dBZ located at a height of 6.1 km ARL (Fig. 11).

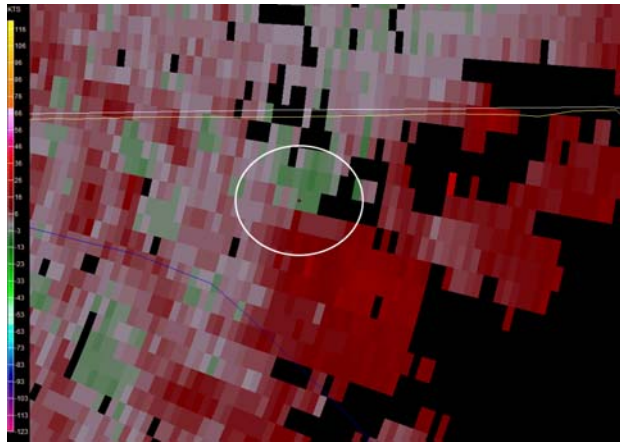

Fig. 10. KFTG 0.5° base velocity for 2130 UTC 23 July 1998. The white circle denotes the circulation associated with the vortex.

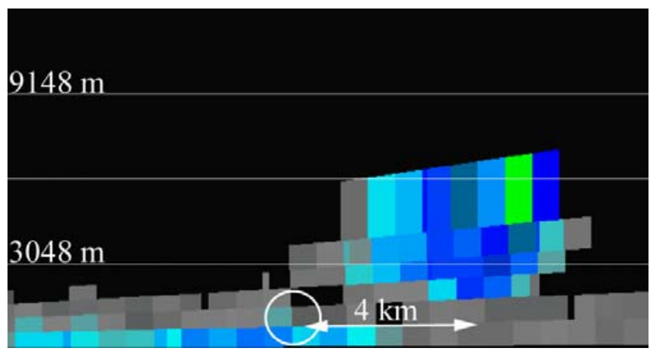

Fig. 11. Base reflectivity cross section from KFTG for 2130 UTC 23 July 1998. Height intervals as in Fig. 4.

Over the next 30 minutes, the velocity couplet associated with the vortex moved east, away from the boundary and became entrained in the storm's updraft. By 2159 UTC the updraft rapidly increased in height with an echo top (5 dBZ) height of 15.2 km ARL. Additionally, the vortex associated with the now ~6 minute old tornado, ascended within the updraft to a height of 3 km ARL (Fig. 12). Furthermore, cross-sectional analysis of the radial velocity data revealed the velocity couplet titled east with height. The tilt with height in the radar data is consistent with the mobile mesonet crew's visual observations of the tornado tilting east with height. At 2205 UTC the largest shear values were resolved associated with the velocity couplet; 28 m s^{-1} across 1.6 km at 1.37 km ARL (Fig. 13). It was near this period in time when the tornado was observed to dissipate. At 2211 UTC the velocity couplet associated with the tornado had nearly dissipated in the volumetric velocity, concurrent at a time when a westward surging outflow boundary produced by the storm undercut the updraft.

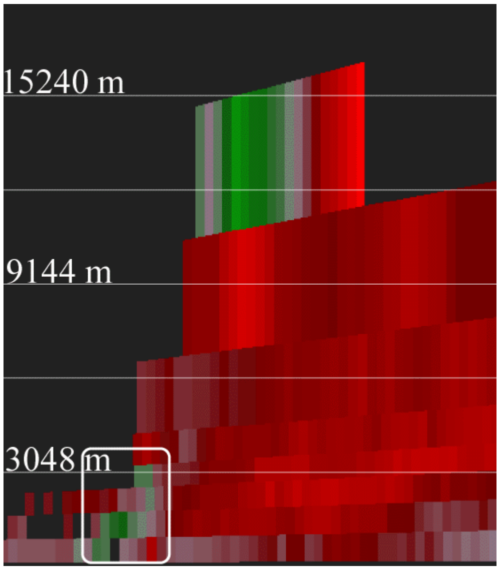

Fig. 12. As in Fig 4 except for 2159 UTC 23 July 1998.

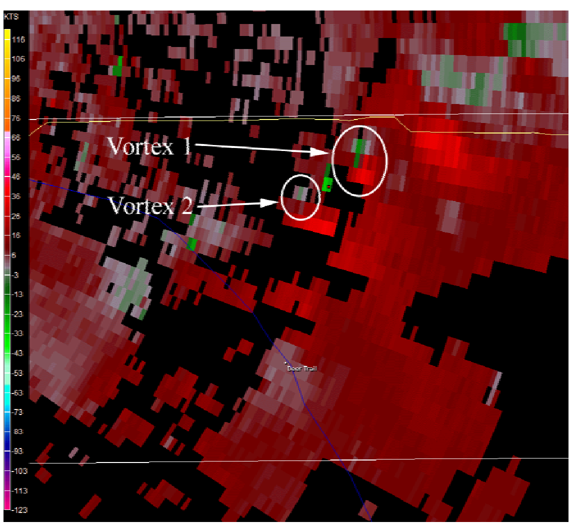

Fig. 13. KFTG 1.5° base velocity 2205 UTC 23 July 1998. The white circles denote vortex locations.

The second vortex associated with the second tornado was much more difficult to resolve in the WSR-88D base data. At 2205 UTC, the vortex that would become entrained in the parent tornadic circulation was resolved, embedded within the DCVZ ~10 minutes before the second tornado (Fig. 13). The circulation trailed 4.5 km southwest of the first vortex. Similar to the first vortex, the depth of the circulation was resolved to a height of ~2 km ARL with a diameter under 1 km. At 2211 UTC, 4 minutes before the tornado, the vortex moved east, off the DCVZ and became collocated with a developing updraft along a flanking line of the same storm that produced the first tornado. The depth of the vortex had increased slightly to 2.4 km ARL with a maximum radial shear of 16 m s^{-1}, 1.4 km ARL (Fig. 14). The velocity signature associated with the parent tornado circulation dissipated by 2223 UTC. The brief duration of the circulation resolved in the base radar data was consistent with the visual observations of the mobile mesonet crew; the second tornado persisted for seven minutes.

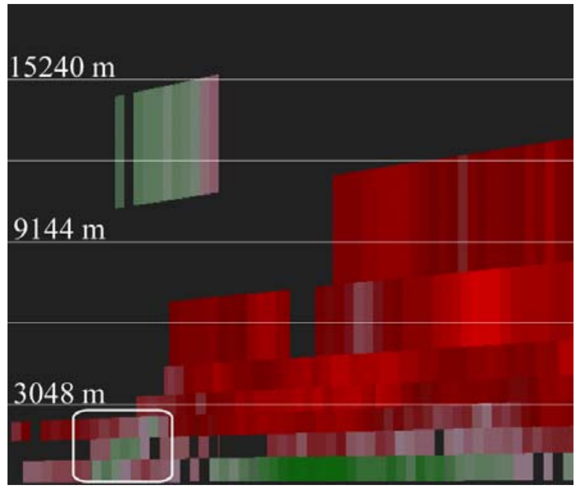

Fig. 14. As in Fig. 4 except for 2211 UTC 23 July 1998.

4. CONCLUDING REMARKS

The three cases presented within demonstrate how WSR-88D base velocity data can resolve pre-existing misocyclones embedded within various surface boundaries through non-mesocyclone tornadogenesis. In several instances, individual vortices could be tracked 120 minutes before becoming collocated with rapidly deepening updrafts. In most instances cross-sectional, reflectivity and velocity data resolved parent circulations associated with the tornadoes, ascending within the parent updrafts prior to tornado genesis. Also common among the cases, the vortices were resolved to be embedded within quasi-stationary surface boundaries and resolved within 85 km from the radars. Additionally, with the 4 October 2004 cases, a lobe and cleft or, rather, an "*S*" shaped pattern could be identified in the base velocity data along the surface boundary concurrent with a train of misocyclones. Although not explicitly discussed, from the cases depicted within and from a plethora of other cases not shown due to space constraints, it was found that base velocity was far superior compared to base reflectivity to resolve misocyclones.

It is noteworthy that numerous non-mesocyclone events that occurred in the Unites States were investigated for possible inclusion in this paper. Of interest, with the vast majority of events that occurred roughly east of 96° longitude, pre-existing misocyclones were not resolved in the base reflectivity or velocity data. We speculate one reason for the lack of detection may be due to insufficient scatterers along the associated low level boundaries as a function of relatively shallow, boundary layer mixing, compared to events where deeper mixing occurred (e.g, > 3 km above ground level). This issue is under investigation.

Provided scatterers are present along surface / low level boundaries to allow sufficient power return back to the WSR-88D, forecasters should monitor WSR-88D base velocity data in order to detect the development of misocyclones, particularly if the mesoβ, or larger, environment is supportive for non-mesocyclone tornadoes (e.g., Davies 2003, Caruso and Davies 2005). To improve the detection and monitoring of misocyclone evolution, it is recommended to utilize the best radar volume coverage pattern that will resolve radar fine lines associated with low level boundaries (e.g. VCP-31, -121), and minimize pulse repetition frequency issues that can arise along and near the boundaries. Additionally, although not explicitly shown, it is highly recommended to use velocity color scales that enhance low velocity values in order to clearly identify shear signatures and flow structure along surface boundaries. Furthermore, cross sectional imagery should be utilized as frequently as plan view imagery to best monitor vortex evolution in terms of rate of ascent, quality of horizontal shear and orientation with height. It is our belief the above recommendations combined with the upcoming release of the WSR-88D Super Resolution Data will foster greater forecaster situational awareness and improve non-mesocyclone tornado warning lead time.

ACKNOWLEDGMENTS

The authors wish to thank Paul Schlatter and Jim Ladue with the Warning Decision Training Branch for providing background data, and Dan Baumgardt with the La Crosse, Wisconsin National Weather Service Forecast Office and Todd Holsten with the North Webster, Indiana National Weather Service Forecast Office for their constructive and insightful comments.

REFERENCES

References available upon request.